

SCIENTIFIC REPORTS



OPEN

Enhancement of electroluminescence from embedded Si quantum dots/SiO₂ multilayers film by localized-surface-plasmon and surface roughening

Received: 03 February 2015

Accepted: 04 June 2015

Published: 03 July 2015

Wei Li^{1,2,3}, Shaolei Wang^{1,2}, Mingyue Hu^{1,2}, Sufeng He^{1,2}, Pengpeng Ge^{1,2}, Jing Wang^{1,2}, Yan Yan Guo^{1,2} & Liu Zhaowei³

In this paper, we prepared a novel structure to enhance the electroluminescence intensity from Si quantum dots/SiO₂ multilayers. An amorphous Si/SiO₂ multilayer film was fabricated by plasma-enhanced chemical vapor deposition on a Pt nanoparticle (NP)-coated Si nanopillar array substrate. By thermal annealing, an embedded Si quantum dot (QDs)/SiO₂ multilayer film was obtained. The result shows that electroluminescence intensity was significantly enhanced. And, the turn-on voltage of the luminescent device was reduced to 3V. The enhancement of the light emission is due to the resonance coupling between the localized-surface-plasmon (LSP) of Pt NPs and the band-gap emission of Si QDs/SiO₂ multilayers. The other factors were the improved absorption of excitation light and the increase of light extraction ratio by surface roughening structures. These excellent characteristics are promising for silicon-based light-emitting applications.

It is well known silicon is an indirect bandgap material. It is not a good choice for light emitting applications. But, it is highly desired to develop Si-based LED materials because of their ease in integrating with the already existing Si integrated circuit technology. And another reason is obviously cost considerations. The other materials, such as GaN, carbon nanotubes and graphene, are expensive for LED. Actually, the researches on silicon nanostructure luminescence began in the 1990s after the discovery of strong visible photoluminescence (PL) from porous silicon at room temperature¹⁻⁴. In addition, it has been reported silicon nanosphere as one kind of all-dielectric materials with low-loss nature and strong magnetic response can induce near-zero reflection and near-perfect transmission^{5,6}. It will be applied in nanophotonics materials. So, it is very important to research the silicon nanomaterials.

Among the many kinds of Si quantum structures, embedded Si quantum dot (QDs)/SiO₂ or embedded Si quantum dot/SiN_x multilayer films have attracted a lot more attention due to its potential application in metal-semiconductor-oxide light emitting diodes⁷⁻¹². In contrast to porous silicon, these films can

¹College of Electronic Science and Engineering, Nanjing University of Posts and Telecommunications, Nanjing, 210003 China. ²Key Laboratory of Radio Frequency and Micro-Nano Electronics of Jiangsu Province, Nanjing 210023, Jiangsu, China. ³Department of Electrical and Computer Engineering, University of California, San Diego, 9500 Gilman Drive, La Jolla, California 92093-0407, USA. Correspondence and requests for materials should be addressed to W.L. (email: Liw@njupt.edu.cn)

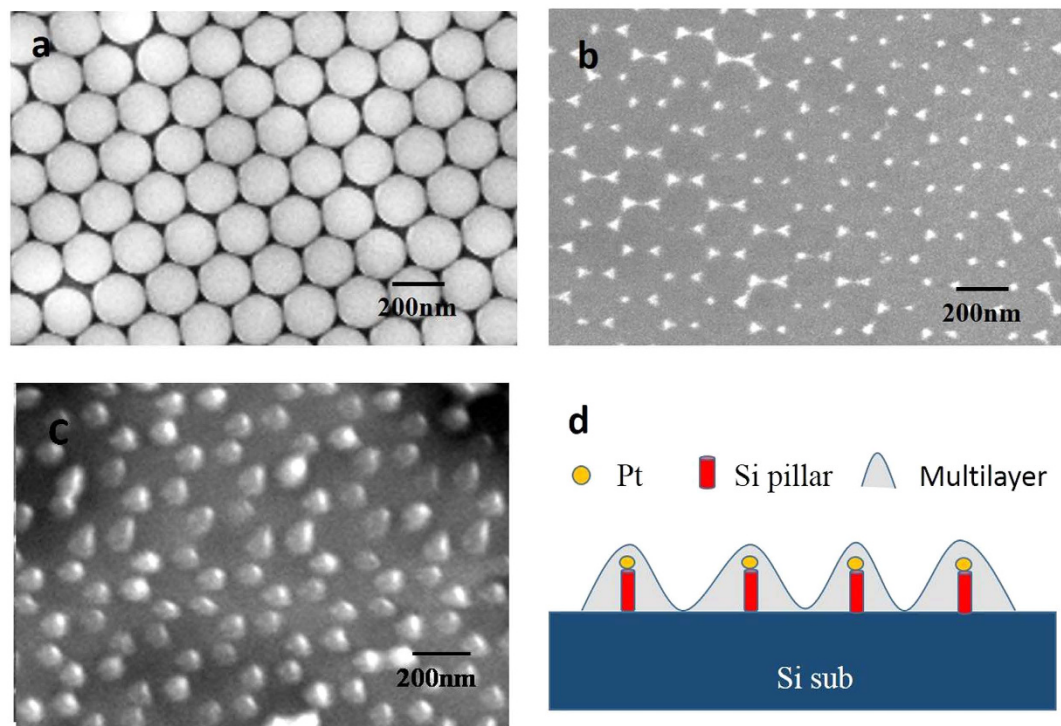


Figure 1. SEM image of single layer of PS spheres (a), Pt nanoparticles (b) Pt nanoparticles coated Si nanopillar (c) and the schematic diagram of electrochromic structures (d).

be obtained on various substrates. Their thickness can range from several nanometers to several microns, which is important in research on the electrochromism.

Despite the huge progress in the luminescence of Si QDs-based system, it is still under investigation for use in optical interconnections in very large scale integration (VLSI). The mechanism of light emission from Si-QDs has been solved due to the observation of the quantum confinement effect (QCE)^{13,14}. It was reported that the light emission of Si-QDs is based on the radiative recombination occurring at surface defect states surrounding the Si-QD core. Another possible principle has attributed the luminescence from the band-to-band transition with Si-QDs to QCE¹⁵. Because of the large difference in refractive index between Si and SiO₂ (or SiN_x), the emission light will be internally reflected at the interface. As a result, the fraction of external light in the Si QDs-based multilayer structures is very small. Many methods, such as introducing photonic crystal structures¹⁶, localized surface plasmon¹⁷ and surface roughening¹⁸ have been applied to address this problem. Localized surface plasmon is one way to enhance light emission due to coupling between the LSP of metallic NPs and the band-gap emission of materials. Surface roughening is another effective way to improve the light extraction ratio by forming the anti-reflection surface and reducing the surface reflection. In this paper, these two methods were both used to enhance the light emission. We prepared a Si QDs/SiO₂ multilayer film on a Pt NPs-coated Si nanopillar array substrate. The Pt NPs were used for their localized surface plasmons and the nanopillar array was used for surface roughening. The result shows that electrochromism intensity was significantly enhanced. And, the turn-on voltage of the luminescent device was reduced to 3 V.

Experiments

(1) Fabrication process of Si nanopillar arrays. The ordered Si nanopillar array substrate was fabricated by nanosphere lithography. It was reported in our previous paper^{19–21}. In the first step, a single layer of polystyrene (PS) spheres with diameter of 220 nm was covered on the P-Si substrate (Fig. 1(a)). Second, a Pt film with 30 nm thickness was deposited on this sample by metal sputtering. After removing the PS spheres, the substrate was dry-etched in reactive ion etching (RIE) system by using 40 sccm CHF₃ gas under RF power of 20 W (Fig. 1(b)). Then, the Pt NP-coated Si nanopillar array was obtained (Fig. 1(c)).

(2) Fabrication process of embedded Si QDs/SiO₂ multilayer. The amorphous Si (a-Si)/SiO₂ multilayer film, composed of 8 pairs of 4 nm a-Si and 4 nm SiO₂ layers, was prepared in the plasma-enhanced chemical vapor deposition (PECVD) system. During the deposition, the rf power and deposition temperature were kept at 35 W and 220°C. The deposition rate is about 0.1 nm/s under the reaction pressure 40 Pa. Silane with a flow rate of 8 sccm was used to deposit amorphous silicon and O₂ with a flow rate of 25

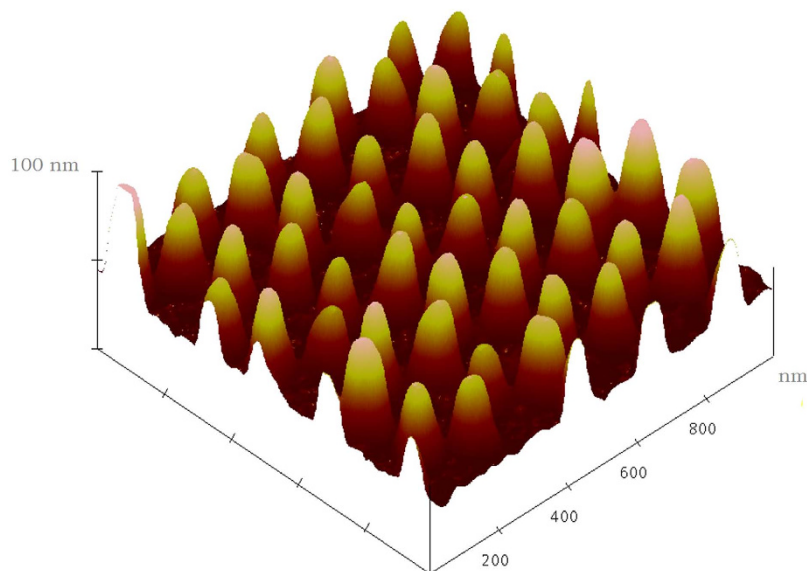


Figure 2. AFM of Pt nanoparticles coated Si nanopillar.

scm was used to oxidize the amorphous silicon layers. Then, the a-Si/SiO₂ multilayer samples were dehydrogenated at 500 °C for 1 hour. After that, they were thermally annealed at 1100 °C for 1 hour to obtain Si QDs/SiO₂ multilayer. Here, an 8-period multilayer film was deposited on Si substrate without nanopillar for comparison. To make electrodes for electroluminescence measurements, Al electrodes were evaporated on the bottom side and the thin ITO electrodes with 1.5 mm in diameter were deposited on the top.

(3) Electroluminescence (EL), extinction and reflection spectra measurement. The measurement of the EL was performed on Fluoromax-2 spectroscopy (Jobin-Yvon) system by applying DC voltage. The spectrum of Pt was performed by using a Shimadzu UV-3600 spectrophotometer in the wavelength range from 200 nm to 700 nm. The typical illuminated area was chosen to be a pinhole with 5 mm diameter. The reflection spectra of front surface were measured by using Shimadzu UV-3600 spectrophotometer for nearly normal light incidence (5% offset) in the wavelength range from 200 nm to 1000 nm.

Result and discussion

Figure 1(a) shows the image of PS spheres monolayer on substrate. It is a classic honeycomb structure. And the area can be as large as $2 \times 2 \text{ cm}^2$. After the sputtering of Pt, we removed all of the PS spheres. Then a very well-ordered triangular array of hexagonal Pt nanoparticles was obtained. It was found in Fig. 1(b). These Pt nanoparticles will be used as a mask in the following etching process. Figure 1(c) is an oblique-view SEM image of the Pt NPs-coated Si pillars. It is shown that periodic Si nanopillars can be obtained by transferring the patterns into silicon substrate. Figure 1(d) is the schematic diagram of electroluminescent structures.

To get more information on the surface morphology, the samples were characterized by atomic force microscopy (AFM). Figure 2 shows the AFM image of embedded Si quantum dots /SiO₂ film on Pt NP-coated Si nanopillar arrays substrate. As can be seen in this image, the pillars are quite uniform. The period constant is 220 nm which corresponds to the diameter of the PS spheres used here. The mean full width at half maximum (FWHM) of the nanopillar is estimated to be 50 nm, with 100 nm height.

Figure 3(a) and Fig. 3(b) show the EL spectra of a Si QDs/SiO₂ multilayer film deposited on substrate without and with the Pt NP-coated nanopillar array. The EL signals were collected when applying DC voltage (from 3 V to 15 V) and it shows that the EL band is quite broad. It looks like that the EL spectra of the sample without Si nanopillar contains at least two sub-bands located at 520 nm and 650 nm, respectively due to the different luminescence routes^{22–25}. This spectra is from QCE in Si nanocrystals and defect-related EL bands in SiO₂-based nanostructures. And these two bands also appear in the EL spectra of the sample with Si nanopillar. As observed from Fig. 3, the EL intensity increases with increased voltage. And the most important is that the EL intensity is obviously enhanced for the sample with Pt NPs-coated Si nanopillar compared to that without Pt NPs-coated Si nanopillar. Figure 4a depicts the normalized integrated EL intensities I_{EL} of the samples with and without Pt NPs-coated Si nanopillar as a function of applied voltage. The I_{EL} of both samples increases with increased voltage. When the applied voltage is 8 V or 10 V, the integrated EL intensities of the sample with Pt NPs-coated Si nanopillars are about 10 times stronger than that of without Pt NPs-coated Si nanopillars. Figure 4b shows the ratio of integrated EL intensity to the injection current as a function of applied voltage for both samples. The ratio of integrated EL intensity to the injection current directly reflects the external quantum efficiency. It

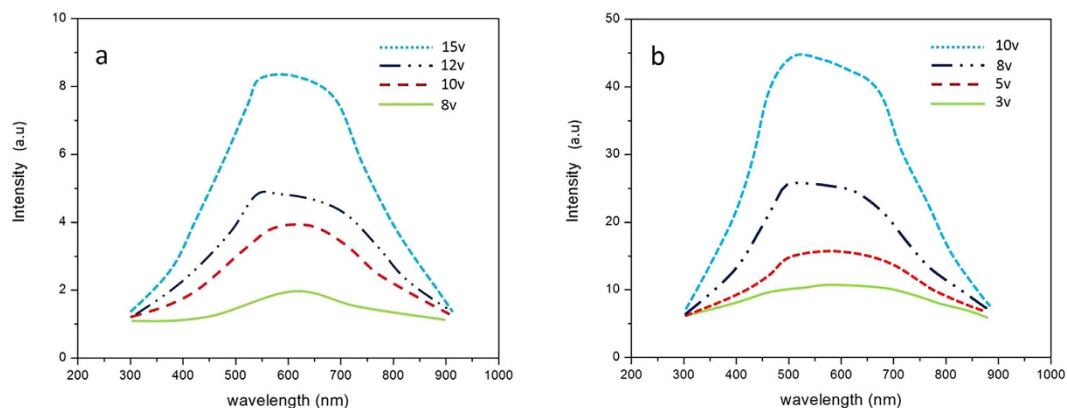


Figure 3. EL spectra of Si QDs/SiO₂ (a) without Pt nanoparticles and Si nanopillar and (b) with Pt nanoparticles coated Si nanopillarsubstrate.

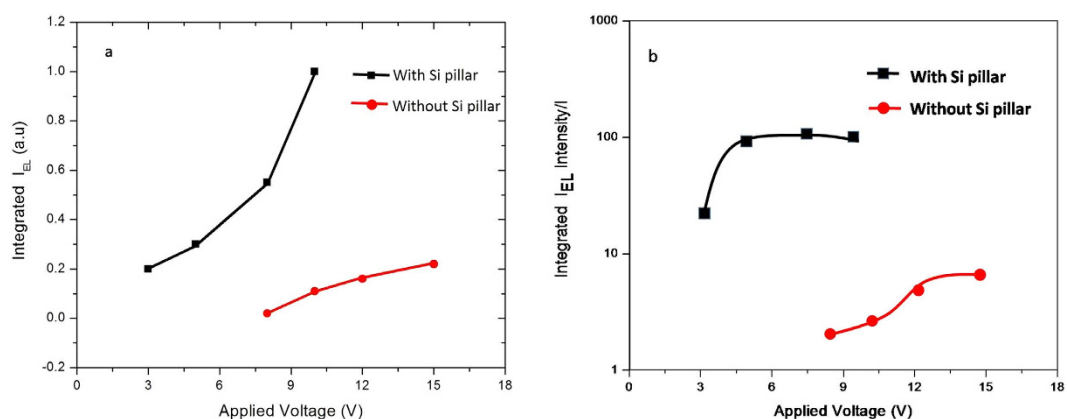


Figure 4. (a) Integrated EL intensity versus the applied DC voltage and (b) efficiency curves as a function of applied voltage .

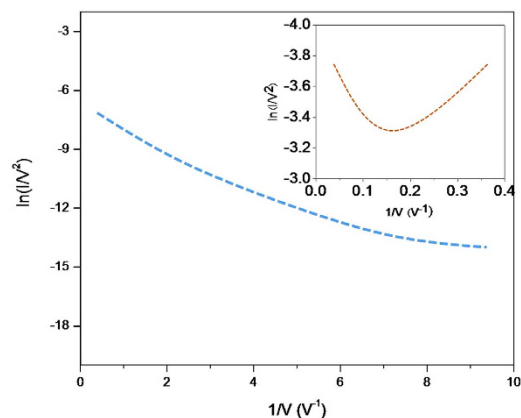


Figure 5. The curves of $\ln(I/V^2)$ and $1/V$ for the samples with pillar. The inset is the curves for the sample without pillar.

is clearly shown that the external quantum efficiency is obviously enhanced for samples with Si pillar. The EL efficiency can be improved by almost two orders of magnitude as shown in Fig. 4(b). It was reported that the EL intensity can be improved due to the enhanced Fowler-Nordheim (F-N) tunneling process by introducing Si interfacial nano-pyramids²⁶. The plots of $\ln(I/V^2)$ vs $1/V$ for both samples are shown in Fig. 5. A nearly linear behavior for the samples with Si nanopillar indicates that the EL follows F-N tunneling mechanism in our case. Meanwile, it is found that the threshold voltage to initiate F-N tunneling

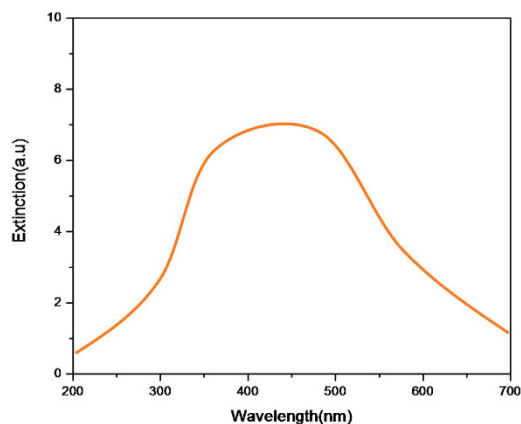


Figure 6. The extinction spectra of Pt nanoparticles.

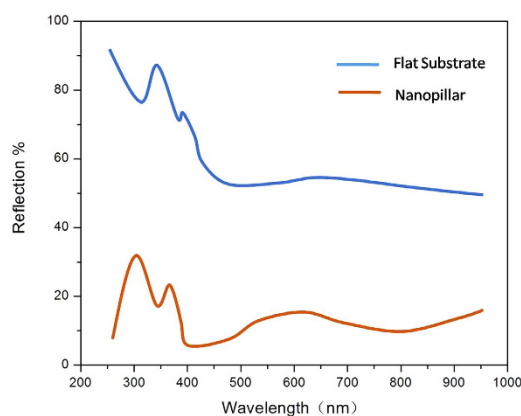


Figure 7. The reflection spectra for flat and nano-patterned Si substrates.

is reduced obviously. The enhancement of the light emission is due to the resonance coupling between the LSP of Pt NPs. When the light emission wavelength of Si QDs/SiO₂ multilayer is close to the extinction peak of Pt nanoparticles, this coupling process occurs. It is reported that the LSP energy of Pt NPs can be tuned in a wide range from the deep-UV to visible region by size control^{27,28}. Figure 6 shows the extinction spectra of Pt nanoparticles. As expected, there is a wide extinction peak in this spectra. And, the FWHM of the peak is around 200 nm. In our researches, the Pt nanoparticle size is in the range of about 40 nm to 80 nm, shown in Fig. 1(b). This is the reason of the wide FWHM. Langhammer has reported that Pt nanoparticles have broader resonance peak and larger nonradiative damping than Au^{29,30}. In our case, the peak of EL spectra from Si QDs is also wide (Fig. 3a). So, the LSP energy of Pt nanoparticle is close to the band-gap emission of the sample. Meanwhile, the larger nonradiative damping make the more energy transfer from Pt nanoparticles to Si QDs. In addition, the better contact between Pt nanoparticles and Si QDs/SiO₂ multilayer is formed after annealing. It is helpful for the LSP coupling.

Another possible explanation for the EL enhancement factor would be the improved surface reflection by Si nanopillars as surface roughening structures. From Erchak's paper, only $1/2n_{eff}^2$ (n_{eff} is the effective refraction index) of light can be extracted from the top³¹. Considering the index of Si and SiO₂, which is about 3.4 and 1.5, it can be estimated that the light escaping from the flat sample without Pt NPs-coated Si nanopillar is 8.3%. As can be seen in Fig. 2, the Si nanopillars have a cone shape, which causes a gradually changing reflective index from top to bottom. And then, the n_{eff} is reduced in the samples with Pt NPs-coated Si nanopillar, which leads to much more light emission. Figure 7 shows the reflection spectra for flat and nano-patterned Si substrates. It is shown that the reflectivity from the front surface of flat Si substrate is above 50% in the whole measurement range. And, it is interesting to find that the light reflection from the front surface is obviously suppressed for the nano-patterned samples, indicating the anti-reflection characteristics for nano-patterned Si substrates. It has been reported enhanced optical absorption was achieved from the Si-based nano-cone or nano-pillar structures and the antireflection³². So the light extraction efficiency can be significantly improved by surface roughing.

Moreover, the turn on voltage was different. Here, the turn on voltage is defined as the voltage at which the EL signal starts to be detected. The turn on voltage is about 8 V for the sample without Pt

NPs-coated Si nanopillar. And it is reduced to 3 V for the sample with Pt NPs-coated Si nanopillar. It is well known that the sharp top of the pillar can lower the surface barrier. And the Pt NPs can supply more electrons. Both of them make the carrier injection into the Si QDs/SiO₂ system easier, thus the EL intensity can be increased.

Conclusion

In conclusion, we prepared an embedded Si quantum dot/SiO₂ multilayer film on a Pt NPs-coated Si nanopillar array. It is found that the light extraction efficiency may be improved due to the LSP of Pt NPs and the surface roughing of Si nanopillars. As a consequence, the EL intensity is increased by 10 times compared with the flat substrate devices and the turn-on voltage is reduced to 3 V. Therefore, it is expected to have important applications in many areas of nanoscience and nanotechnology.

References

- Canham, L. T. Silicon quantum wire array fabrication by electrochemical and chemical dissolution of wafers. *Appl. Phys. Lett.* **57**, 1046 (1990).
- Park, N.-M., Choi, C.-J., Seong, T.-Y. & Park, S.-J. Quantum Confinement in Amorphous Silicon Quantum Dots Embedded in Silicon Nitride. *Phys. Rev. Lett.* **86**, 1355 (2001).
- Nguyen, P. D., Kepaptsoglou, D. M., Ramasse, Q. M. & Olsen, A. Direct observation of quantum confinement of Si nanocrystals in Si-rich nitrides. *Phys. Rev. B* **85**, 085315 (2012).
- de Boer, W. D. A. M. *et al.* Red spectral shift and enhanced quantum efficiency in phonon-free photoluminescence from silicon nanocrystals. *Nat. Nanotech.* **5**, 878–884 (2010).
- Jiahao, Y. *et al.* Directional Fano Resonance in a Silicon Nanosphere Dimer. *ACS Nano* **9**, 2968–2980 (2015).
- Jiahao, Y. *et al.* Magnetically induced forward scattering at visible wavelengths in silicon nanosphere oligomers. *Nat. Commun.* **6**, 7042 (2015).
- Heitmann, J., Muller, F., Zacharias, M. & Gosele, U. Silicon Nanocrystals: Size Matters. *Adv. Mater.* **17**, 795–803 (2005).
- Gourbilleau, F. *et al.* Silicon-rich SiO₂/SiO₂ multilayers: A promising material for the third generation of solar cell. *J. Appl. Phys.* **106**, 013501 (2009).
- Daldosso, N. & Pavesi, L. Nanosilicon photonics. *Laser & Photon. Rev.* **3**, 508–534 (2009).
- Marconi, A. *et al.* High power efficiency in Si-nc/SiO₂ multilayer light emitting devices by bipolar direct tunneling. *Appl. Phys. Lett.* **94**, 221110 (2009).
- Lin, Y. H., Wu, C. L., Pai, Y. H. & Lin, G. R. A 533-nm self-luminescent Si-rich SiN_x/SiO_x distributed Bragg reflector. *Opt. Express* **19**, 6563–6570 (2011).
- Tai, H. Y., Lin, Y. H. & Lin, G. R. Wavelength-Shifted Yellow Electroluminescence of Si Quantum-Dot Embedded 20-Pair SiN_x/SiO_x Superlattice by Ostwald Ripening Effect. *IEEE Photon. J.* **5**, 6600110 (2013).
- Koch, F., Petrova-Koch, V. & Muschik, T. The luminescence of porous Si: the case for the surface state mechanism. *J. Lumin.* **57**, 271–281 (1993).
- Prokes, S. M. Light emission in thermally oxidized porous silicon: Evidence for oxide-related luminescence. *Appl. Phys. Lett.* **62**, 3244–3246 (1993).
- Delley, B. & Steigmeier, E. F. Quantum confinement in Si nanocrystals. *Phys. Rev. B Condens. Matter* **47**, 1397–1400 (1993).
- Kim, B. H. *et al.* Enhancement of the External Quantum Efficiency of a Silicon Quantum Dot Light-Emitting Diode by Localized Surface Plasmons. *Adv. Mater.* **20**, 3100–3104 (2008).
- Mochizuki, Y. *et al.* Enhancement of photoluminescence from silicon nanocrystals by metal nanostructures made by nanosphere lithography. *J. Appl. Phys.* **106**, 013517 (2009).
- Kang, Z. T. *et al.* Enhancement of white luminescence from SiN_x films by surface roughening. *Nanotechnology* **18**, 415709 (2007).
- Li, W. *et al.* Fabrication of large-scale periodic silicon nanopillar arrays for 2D nanomold using modified nanosphere lithography. *Appl. Surf. Sci.* **253**, 9035–9038 (2007).
- Li, W. *et al.* Field emission from a periodic amorphous silicon pillar array fabricated by modified nanosphere lithography. *Nanotechnology* **19**, 135308 (2008).
- Li, W. *et al.* Humidity sensing properties of morphology-controlled ordered silicon nanopillar. *Appl. Surf. Sci.* **317**, 970–973 (2014).
- Pucker, G. *et al.* (Si/SiO₂)_n multilayers and microcavities for LED applications. *Opt. Mater.* **17**, 27–30 (2001).
- Lin, G. R., Lin, C. J. & Lin, C. K. Oxygen defect and Si nanocrystal dependent white-light and near-infrared electroluminescence of Si-implanted and plasma-enhanced chemical-vapor deposition-grown Si-rich SiO₂. *J. Appl. Phys.* **97**, 094306 (2005).
- Glinka, Yu. D., Lin, S. H., Hwang, L. P. & Chen, Y. T. Photoluminescence from mesoporous silica: Similarity of properties to porous silicon. *Appl. Phys. Lett.* **77**, 3968–3970 (2000).
- Zyubin, A. S. *et al.* Red and near-infrared photoluminescence from silica-based nanoscale materials: Experimental investigation and quantum-chemical modeling. *J. Chem. Phys.* **116**, 281 (2002).
- Chen, H., Lien, Y. C., Wu, C. L. & Lin, G. R. Multicolor electroluminescent Si quantum dots embedded in SiO_x thin film MOSLED with 2.4% external quantum efficiency. *Opt. Express* **21**, 391–403 (2013).
- Bigall, N. C. *et al.* Monodisperse Platinum Nanospheres with Adjustable Diameters from 10 to 100 nm: Synthesis and Distinct Optical Properties. *NanoLett.* **8**, 4588–4592 (2008).
- Lin, G. R., Lin, C. J. & Kuo, H. C. Improving carrier transport and light emission in a silicon-nanocrystal based MOS light-emitting diode on silicon nanopillar array. *Appl. Phys. Lett.* **91**, 093122 (2007).
- Langhammer, C., Yuan, Z., Zoric, I. & Kasemo, B. Plasmonic Properties of Supported Pt and Pd Nanostructures. *NanoLett.* **6**, 833–838 (2006).
- Zoric, I., Zach, M., Kasemo, B. & Langhammer, C. Gold, Platinum, and Aluminum Nanodisk Plasmons: Material Independence, Subradiance, and Damping Mechanisms. *ACS Nano* **5**, 2535–2546 (2011).
- Erchak, A. A. *et al.* Enhanced coupling to vertical radiation using a two-dimensional photonic crystal in a semiconductor light-emitting diode. *Appl. Phys. Lett.* **78**, 563–565 (2001).
- Zhu, J. *et al.* Optical absorption enhancement in amorphous silicon nanowire and nanocone arrays. *Nano Lett.* **9**, 279–282 (2009).

Acknowledgments

This work is supported by National Natural Science Foundation of China (No.51302136 and No.11304158), Natural Science Foundation of Jiangsu Province Universities (No. 12KJB510016) and Jiangsu Province College Graduate Research and Innovation Projects (No.CXLX13_454).

Author Contributions

Li W. and Wang S.L. conceived the idea. He S.F., Wang J. and Guo Y.Y. performed the experiment. Hu M.Y., Ge P.P. and Liu Z.W. contributed to the theory. All authors analyzed the result and contributed to the article.

Additional Information

Competing financial interests: The authors declare no competing financial interests.

How to cite this article: Li, W. *et al.* Enhancement of electroluminescence from embedded Si quantum dots/SiO₂ multilayers film by localized-surface-plasmon and surface roughening. *Sci. Rep.* **5**, 11881; doi: 10.1038/srep11881 (2015).



This work is licensed under a Creative Commons Attribution 4.0 International License. The images or other third party material in this article are included in the article's Creative Commons license, unless indicated otherwise in the credit line; if the material is not included under the Creative Commons license, users will need to obtain permission from the license holder to reproduce the material. To view a copy of this license, visit <http://creativecommons.org/licenses/by/4.0/>